Article

Osteogenesis or Apoptosis—Twofold Effects of Zn²⁺ on Bone Marrow Mesenchymal Stem Cells: An In Vitro and In Vivo Study

Yu Liu, Linbang Wang, Xinyu Dou, Mingze Du, Shuyuan Min, Bin Zhu,* and Xiaoguang Liu*

Cite This: *ACS Omega* 2024, 9, 10945–10957

Read Online

ACCESS | 📊 Metrics & More | 📖 Article Recommendations | 🆘 Supporting Information

ABSTRACT: Zinc (Zn) is a bioabsorbable metal that shows great potential as an implant material for orthopedic applications. Suitable concentrations of zinc ions promote osteogenesis, while excess zinc ions cause apoptosis. As a result, the conflicting impacts of Zn^{2+} concentration on osteogenesis could prove to be significant problems for the creation of novel materials. This study thoroughly examined the cell viability, proliferation, and osteogenic differentiation of rat bone marrow mesenchymal stem cells (rBMSCs) cultured in various concentrations of Zn^{2+} in vitro and validated the osteogenesis effects of zinc implantation in vivo. The effective promotion of cell survival, proliferation, migration, and osteogenic differentiation of bone marrow mesenchymal stem cell (BMSCs) may be achieved at a low concentration of Zn^{2+} (125 μM). The excessively high concentration of zinc ions (>250 μM) not only reduces BMSCs' viability and proliferation but also causes them to suffer apoptosis due to the disturbed zinc homeostasis and excessive Zn^{2+}. Moreover, transcriptome sequencing was used to examine the underlying mechanisms of zinc-induced osteogenic differentiation with particular attention paid to the PI3K-AKT and TGF-β pathways. The present investigation elucidated the dual impacts of Zn^{2+} microenvironments on the osteogenic characteristics of rBMSCs and the associated processes and might offer significant insights for refining the blueprint for zinc-based biomaterials.
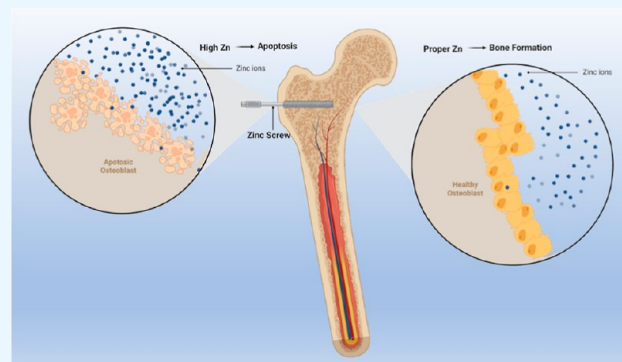
1. INTRODUCTION

Metallic materials are frequently used in orthopedics. Stainless steel, cobalt−chromium (Co−Cr), titanium (Ti), and other alloys are examples of traditional nonbiodegradable metallic biomaterials for orthopedics that are often utilized as permanent or temporary implants to restore function by supporting hard tissues.[1] However, there are some problems with nonbiodegradable materials such as immune response, peri-implant stress shielding, difficulty in revision surgery, implant-related infections or rupture, which can cause great suffering to patients.[2] Thus, the idea of biodegradable metal for implants was put up, which states that biodegradable metallic materials can dissolve entirely during tissue healing and corrode progressively in vivo due to bodily fluids.[3] In the process, the patient has less discomfort; there is less chance of a second operation to remove the implant, and the expense of medical care is decreased as the load is progressively passed to the healing tissues.

Iron-, zinc-, and magnesium-based metallic compounds are now the most common types of biodegradable metallic materials. Over the last 10 years, a great deal of research has been done on medical degradable magnesium and iron alloys.[4] But it has been discovered that magnesium degrades too quickly, and that this rapid deterioration is accompanied by the generation of hydrogen; the former leads to an excessive loss of function, while the latter prevents healing.[5] Conversely, the rate of iron breakdown is too sluggish and the degradation products are stored in the body for an extended duration, which is harmful to tissue regeneration. Zinc degrades at a pace that is halfway between that of magnesium and iron, does not release hydrogen throughout the process, and the body can fully absorb the byproducts.[6,7] Besides, zinc ions play a crucial role in the energy metabolism of bone cells and are necessary cofactors for important enzymes connected to bone metabolism, such as collagenase, alkaline phosphatase (ALP), and carbonic anhydrase.[8,9] Zinc ions exhibit favorable osteogenic activity by enhancing osteoblast mineralization and proliferation, as well as by encouraging the expression of osteoblast marker genes and the production of collagen by bone marrow mesenchymal stem cells (BMSCs).[10−12] Therefore, zinc is a better biodegradable metallic substance than iron and magnesium.

Compared with magnesium alloy, zinc alloy has the advantages of slow degradation and no hydrogen production

during the degradation process, which is expected to become ideal biodegradable orthopedic implant material. However, zinc alloys are not as biocompatible as magnesium. Although zinc is superior to magnesium in terms of degradation properties, it is inferior to magnesium in terms of biocompatibility. The human's need for zinc intake is much smaller than magnesium; the recommended daily intakes of magnesium and zinc are 375−700 and 6.5−15 mg, respectively.[13] Similarly, cells are much less tolerant to zinc ions than to magnesium ions. For osteoblast cells, the LD50s for zinc and magnesium ions, respectively, were 0.09 and >4.02 mmol/L,[14] and high concentrations of zinc ions can cause cell death and cytotoxic responses.[15,16] Therefore, zinc ions have both benefits and drawbacks for bone development, though.

Given the dual roles of zinc in bone regeneration and cytotoxicity, when designing zinc implant materials, the adverse effects of zinc ions should be avoided as much as possible. It is imperative to thoroughly assess both positive and negative effects of the Zn^{2+} microenvironments on osteogenesis and to elucidate the relevant processes in order to precisely manage and optimize Zn^{2+} release. This study thoroughly examined the cell viability, proliferation, and osteogenic differentiation of BMSCs cultured in various concentrations of Zn^{2+}, exploring appropriate Zn^{2+} concentrations that can stimulate the growth and osteogenic differentiation of BMSCs in vitro, and validating the osteogenesis effect of zinc implantation in vivo. Furthermore, the underlying processes of zinc-induced osteogenic differentiation were investigated by transcriptome sequencing, with a focus on the TGF-β pathway and the PI3K-AKT pathway. This study might shed light on the guidance of the development of biodegradable zinc implants for orthopedic applications.

2. MATERIALS AND METHODS

2.1. Cell Isolation and Culture. All animal operations were carried out in compliance with Peking University's guidelines for the care and use of laboratory animals, and they were all approved by the Peking University Third Hospital's animal ethics committee. In the following experiments, rat bone marrow mesenchymal stem cells (rBMSCs) were employed. According to previously reported procedures,[17] the rBMSCs were extracted from the 4-week-old Sprague−Dawley (SD) rats' femur. The rBMSCs were incubated in α-minimum essential medium (α-MEM, Gibco, USA) with 10% fetal bovine serum (FBS, Viva Cell Biosciences, China) and 1% penicillin and streptomycin (Hyclone, USA) at 37 °C in a 5% CO_2 incubator. The rBMSCs were cultured in five distinct types of culture media with various concentrations of $ZnCl_2$ (Macklin, China) to ascertain the impact of various Zn^{2+} microenvironments on the rBMSCs. Five groups were utilized in the experiment: one served as the control group (α-MEM without Zn^{2+}), and the other four served as the experimental groups (α-MEM with Zn^{2+} concentrations of 50, 125, 250, and 500 μM, respectively).

2.2. Cell Viability. Cell viability was detected by a cell counting kit-8 (CCK-8, Yeason, China). First, rBMSCs were incubated in the 98-well plates at a density of 5000 per well in α-MEM without Zn^{2+}. After 12 h, the medium was replaced by fresh α-MEM (control group) or α-MEM with Zn^{2+} concentrations of 50, 125, 250, and 500 μM (experimental groups). The 96-well plate was subsequently incubated at 37 °C and 5% CO_2 for 1, 3, and 5 days with six parallel wells in each group. Fresh media containing 10% CCK-8 solution was added at the respective detection time points, and the cells were then incubated at 37 °C for 2 h. The O.D. value was detected at a wavelength of 450 nm, and the cell viability was calculated following the manufacturer's recommendations.

2.3. Live−Dead Staining. In the 48-well plates, rBMSCs were cultured at a density of 1×10^4 cells per well. After 12 h, the medium was changed to fresh α-MEM or α-MEM included 50, 125, 250, or 500 μM of Zn^{2+}. Three days later, the live−dead staining kit (Yeason, China) was employed to evaluate the vitality of the cells after 3 days. Propidium iodide (4 μM) and Calcein-AM (2 μM) were both included in the live−dead staining solution. The staining solution was added to the medium according to the instruction, which was then incubated for 1 h at room temperature. These samples were looked at using a confocal laser fluorescence microscope (CLSM, Leica, German), where living cells show up as green and dead cells as red, after three PBS washes.

2.4. Cytoskeleton Morphology. To investigate the effect of different concentrations of zinc ions on rBMSCs' morphology, F-actin was stained by phalloidin. The samples were prepared as discussed in Section 2.3. The working solution was made by aspirating 4 mL of 1% PBS-BSA solution into 4 μL of iFluor 488 phalloidin (Yeason, China), at a concentration of 100 μmol/L. Before being fixed in 4% paraformaldehyde for 30 min at room temperature and permeabilized for 5 min with 0.1% TritonX-100 solution, the cells were first washed three times with PBS, followed by two additional PBS washes. After the cells had been stained with the aforementioned working solution for 60 min at room temperature, two PBS washes, and a subsequent 5 min in DAPI solution (Solarbio, China) at room temperature, the cytoskeleton morphology was then evaluated under the CLSM.

2.5. Flow Cytometry. Apoptosis was identified using the Annexin V-FITC Apoptosis Detection Kit (Beyotime, China) in the presence of various Zn^{2+} concentrations. In 6-well plates, rBMSCs were first seeded for 12 h before the medium was changed to α-MEM containing 50, 125, 250, or 500 μM of Zn^{2+}. Following the aforementioned kit's instructions, the flow cytometer (CytoFLEX S, Bechman Coulter, USA) was used to identify the rBMSCs' apoptosis 3 days later.

2.6. Cell Migration. From the results of the previous experiments, it can be seen that when the concentration of zinc ions exceeds 250 μM, the cell viability will be adversely affected, so the subsequent experiments used concentrations of zinc ions of 50 and 125 μM to treat the rBMSCs in order to investigate the effects of zinc ions on physiological functions. rBMSCs were first seeded into a 6-well plate (1×10^4 cells/well), when the cells had achieved 90% confluence, and a linear scratch was then created. PBS was used to wash and remove floating cells, and normal media, media with 50 μM Zn^{2+}, or media with 125 μM Zn^{2+} were employed as culture medium replacements. A digital inverted microscope was used to track the migration of cells into the wound after an additional 48 h. The percentage of the initial wound migration path that migrating cells covered was used to gauge the degree of scratch closure.

2.7. ALP Staining and Activity Testing. Five-hundred microliters of rBMSCs suspension were injected into 48-well plates at a density of 5×10^3 cells/mL, and the culture conditions were changed to either normal control, media with 50 mol/L Zn^{2+}, or media with 125 μM Zn^{2+} in osteogenic differentiation media. The cells were cultivated for 7 days at 37 °C in a cell culture incubator with fluid refreshed every 3 days.

Table 1. Osteogenic-Related Gene Sequence for qRT-PCR

gene	forward primer (5′−3′)	reverse primer (5′−3′)
Runx-2	ACCATGGTGGAGATCATCGC	GGTGGGGAGGATTGTGTCTG
BMP-2	CGGGAACAAATGCAGGAAGC	AAGGACATTCCCCATGGCAG
ALP	CGGCTGGAGATGGACAAGTT	AATGCTGATGAGGTCCAGGC
OPN	GCTAGCCTCAAACTCACGGT	GCTGTTTCAGACGGTCTCCA
OCN	GAGGACCCTCTCTCTGCTCA	AAGAGGCTCCAGGGTCCTAG
COL1	TAGGAGTCGAGGGACCCAAG	AGGCTCTCCCTTAGGACCAG

After three PBS washes, 4% paraformaldehyde was added, and it was left to rest at room temperature for 30 min to test the viability of the cells using a BCIP/NBT Alkaline Phosphatase Staining Kit (Beyotime, China). The appropriate amount of the working solution for the BCIP/NBT ALP staining was prepared and placed into a 48-well plate. The plates were then exposed to light-free incubation at room temperature for 30 min. Under a microscope, the ALP's color shift was seen. A BCA Protein Quantification Kit (Yeason, China) was used to measure the protein content after cells were placed in different media for 14 days. Cells were cleaved using a RIPA lytic solution (Beyotime, China). ALP activity was measured using an Alkaline Phosphatase Test Kit (Beyotime, China), and the relative activity was standardized by protein concentration.

2.8. Alizarin Red S (ARS) Staining and Quantitative Analysis. As discussed in Section 2.7, rBMSCs were incubated in osteogenic differentiation media with various concentrations of Zn^{2+} for 21 days. The cells were then fixed with 4% paraformaldehyde for 20 min followed by three PBS washes. A microscope was used to study calcium nodules after they had been treated with an Alizarin Red Staining Kit (Beyotime, China). After scanning, the staining was extracted using 10% (w/v) cetylpyridinium chloride (Sigma-Aldrich, USA) for quantification. The extract liquor's absorbance was measured using spectrophotometry at 570 nm.

2.9. qRT-PCR. Using the Steady Pure Universal RNA Extraction Kit (Accurate Biology, China), total RNA was extracted after exposure to varied Zn^{2+} concentrations for 14 days. To get cDNA for qPCR, the Evo M-MLV RT Premix for qPCR Kit (Accurate Biology, China) was utilized. SYBR Green Premix Pro Taq HS qPCR Kit (Accurate Biology, China) was used for the qPCR procedure. The real-time PCR primer sequences designed are shown in Table 1.

2.10. Western Blot. Similar to Section 2.9, rBMSCs were grown in various culture media for 14 days. rBMSCs were lysed in ice-cold RIPA buffer and centrifuged at 12,000 rpm for 15 min at 4 C to extract the total protein. A BCA protein assay kit (Yeason, China) was used to quantify the proteins. The protein samples (10 mg) were separated using sodium dodecyl sulfate polyacrylamide gel electrophoresis (SDS-PAGE, Biotides, China), and then, they were transferred to PVDF membranes with 0.45 μm pore sizes (Millipore, German). The membranes were incubated overnight at 4 °C with anti-collagen I (1:1000, Abcam, UK), anti-Runx-2 (1:1000, Abcam, UK), anti-Osterix (1:1000, Abcam, UK), anti-Osteopontin (1:1000, Abcam, UK), anti-BMP-2 (1:1000, Abcam, UK), anti-p-Smad (1:1000, CST, USA), anti-Smad (1:1000, CST, USA), anti-p-AKT (1:1000, Abcam, UK), anti-AKT (1:1000, Abcam, UK) and anti-β-Actin (1:2000, Applygen, China) in the blocking buffer after being blocked with 0.1% tween containing 5% nonfat dry milk solution for 1 h at room temperature. Using an enhanced chemiluminescence detection system (Tenda, China), particular protein bands were seen after

being treated with the HRP marked secondary antibodies (1:10,000, Applygen, China) for 1 h. β-Actin protein expression was employed as an endogenous control for normalization in Western blot analysis.

2.11. Animal Experiment. Titanium alloy screws (diameter: 1.5 mm, length: 6 mm) were purchased from Shandong Kangsheng Medical Device Company. A pure zinc rod was purchased from Hefei Weng Hou Metal Materials Company (diameter: 1 cm, length: 1 m), and the zinc rod was sent to Changzhou Wentuo Medical Device Company to be processed into screws (diameter: 1.5 mm, length: 6 mm). According to a previous study,[18] the pure zinc screw samples were obtained by incubating equal mass (1 g) in 10 mL of α-MEM media for 24 h and then filtering with 0.22 μm filters, and the concentration of zinc ions in the extractions were detected by ICP−MS (inductively coupled plasma mass spectrometry). Then the extracts were diluted to 50 and 10% and the cell viability is measured as in 2.2. According to ASTM G31-12a, immersion test was performed in simulated body fluid (SBF) solution for 168 h. Pure zinc samples with a surface area of 3 cm^2 were immersed in 60 mL of SBF solution at 37 °C, and then the SBF solution was renewed every 48 h. The concentration of zinc ions in the SBF were detected by ICP−MS (inductively coupled plasma mass spectrometry) every day. Two types of screws were sterilized and were ready for use. All the animal experiments were approved by the Animal Care and Experiment Committee of Peking University Third Hospital. Twenty-four 8 week-old male SD Rats were used. All rats were randomly separated into two groups according to implant materials: 12 rats for the Ti6Al4 V screw and 12 for pure zinc screw. The rats were anesthetized with 2% pentobarbital sodium saline solution (0.3 mL/100 g). The left leg was shaved, depilated, and disinfected with iodine. Then the rats were placed in the supine position, with the femur covered by a sterile drape to provide sterile conditions during surgery. A 0.5 cm longitudinal lateral parapatellar incision was made across the knee. After the femoral condyle was exposed, a 1.0 mm hole was drilled into the medial femoral condyle from the top of the lateral epicondyle to the medial epicondyle. The screw was implanted after countersinking by a 1.5 mm drill bit. Silk sutures were used to bind the skin and subcutaneous tissue together in layers. Each rat received 160,000 units of penicillin intramuscularly every 3 days to prevent postoperative infection. Following the surgery, all rats were observed everyday for indications of severe limping, infection, development of subcutaneous emphysema, exposure to screws, and appetite loss.

2.12. Microcomputed Tomography (MicroCT) Analysis. Twelve weeks after surgery, the rats were sacrificed and the left femurs were removed and preserved with 4% paraformaldehyde. Rat femoral condyle specimens were subjected to a microCT scan (Inveon Scanners, Siemens, Germany) with an integration time of 314 ms, a voltage of 55
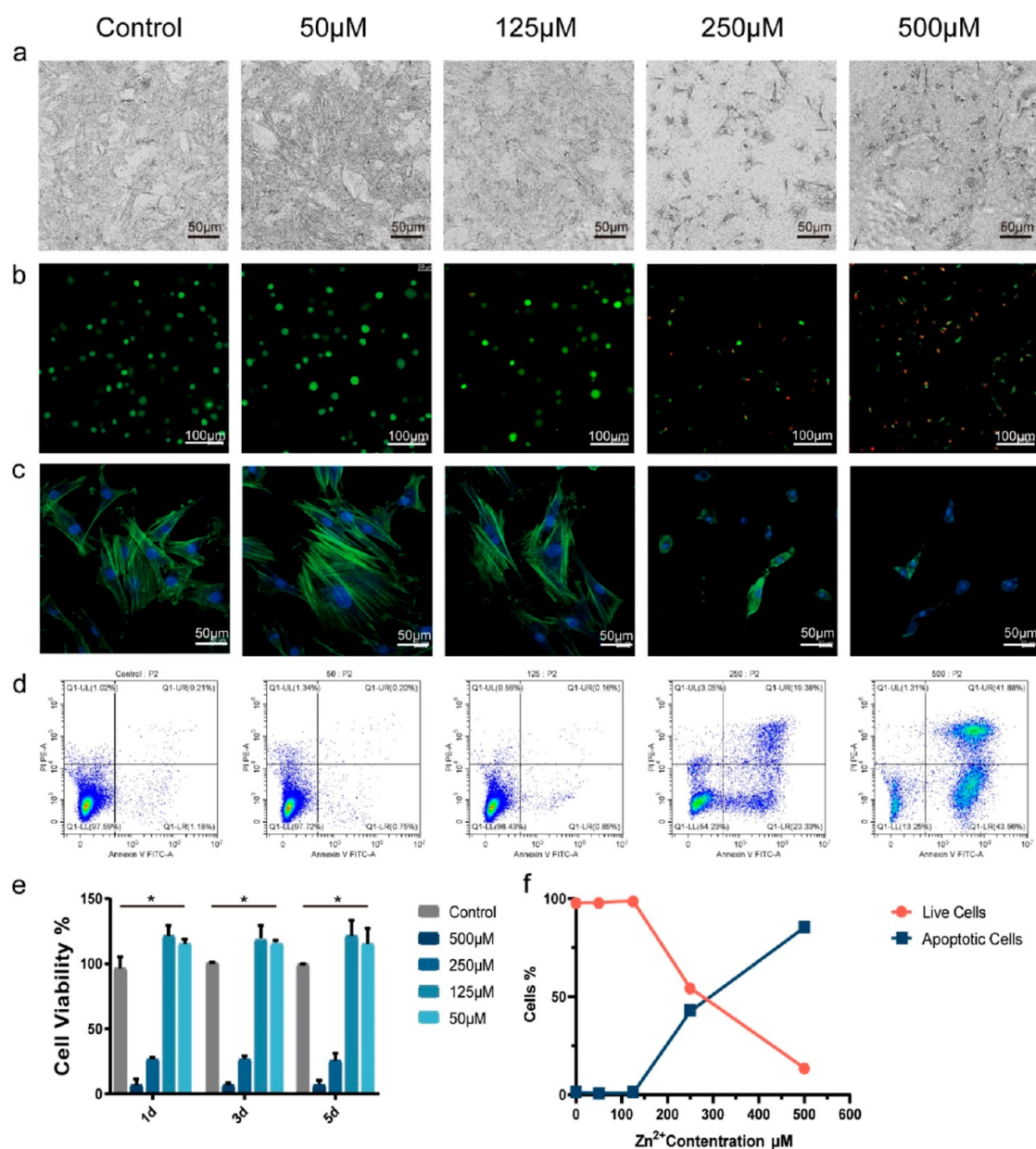
Figure 1. Effects of different concentrations of zinc ions on cell morphology, viability, and apoptosis. (a) The morphology rBMSCs treated with different concentrations of zinc ions for 24 h. (b) Live−dead staining images of rBMSCs (green: live cells, red: dead cells) cultured in various concentrations of zinc ions for 3 days. (c) Cytoskeleton images of rBMSCs exposed to various concentrations of zinc ions for 3 days (green: actin, blue: nuclei). (d) Apoptosis test of rBMSCs treated with different concentrations of zinc ions for 3 days. (e) Cell viability of rBMSCs cultured in various concentrations of zinc ions for 1 day, 3 days, and 5 days. (*$P > 0.05$). (f) Proportion of living and apoptotic cells detected by flow cytometry.

kV, and a current of 145 mA after the surface soft tissue was removed. The new bone tissue was examined by using analytic software (Inveon Research Workplace, Siemens, Germany). The circular bone tissue around the intramedullary nails was identified as the region of interest. The following osteogenesis parameters were quantitatively analyzed for the return on investment: Tb.N (trabecular number), Tb.Th (trabecular thickness), Tb.Sp (trabecular separation), and BV/TV (percentage of the bone volume to total volume).

2.13. Histological Evaluation. Slices of hard and soft tissues were generated after the microCT scan. The specimens were rinsed with water, dehydrated with ethanol, cleaned with xylene, and then embedded with methyl methacrylate for hard-tissue slicing (with implants). The long axis of the femur was parallel to the cutting direction. Subsequently, slices underwent methylene blue acidic magenta staining. Following decalcification, the specimens were embedded in paraffin for soft-tissue slices (without implants). Following the established methods, the expression of Col-1, OPN, and Runx-2 was assessed simultaneously by immunohistochemistry and immunofluorescence staining.

2.14. Transcriptome Sequencing. BMSCs treated with osteogenic induction medium without and with zinc ions (concentration of 125 μM) for 7 days were suitably solubilized in TRIZOL (Thermo, USA). The extracted RNA was reverse-transcribed to create a cDNA library for Illumina platform sequencing once the RNA quality control was finished. Beijing Genomics Institution Multi-Organomics System (https://
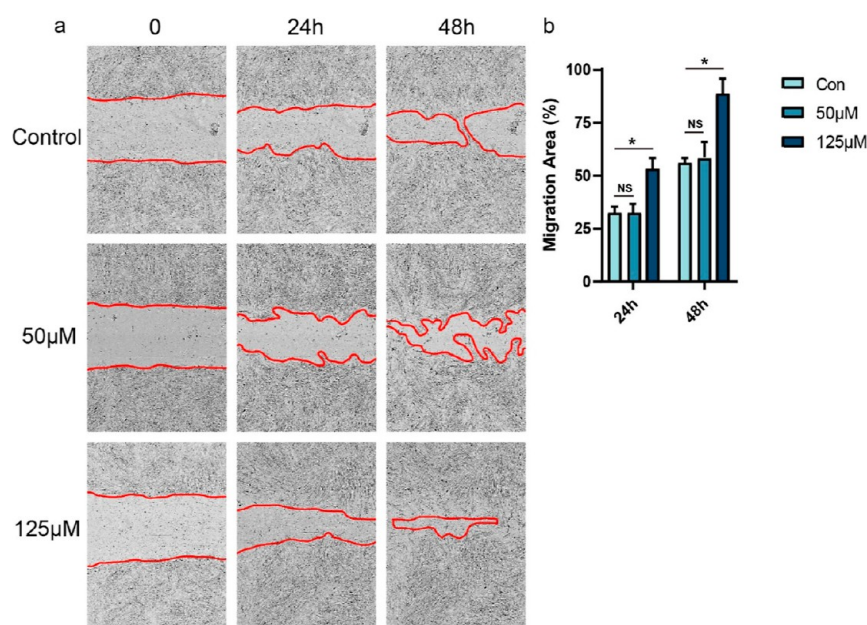
Figure 2. Effects of different concentrations of zinc ions on migration of BMSCs. (a) Migration assay of BMSCs treated with different concentrations of zinc ions. (b) The migration area of BMSCs (*$P < 0.05$).

biosys.bgi.com) was utilized for the bioinformatic analysis of differentially expressed genes (DEGs).

2.15. Statistical Analysis. The mean and standard deviation from six parallel samples are used to illustrate the results. A double-tail Student's t-test was used to see how much the two sets of data differed statistically. To examine the statistical differences between two or more groups, a one-way ANOVA was employed. Software called SPSS 20.0 software (IBM, New York, NY, USA) was used to analyze the data. To ascertain if the data were significant, p-values of less than 0.05 were employed.

3. RESULTS AND DISCUSSION

3.1. Effects of Different Concentrations of Zinc Ions on Activity, Morphology and Apoptosis of BMSCs. As a biodegradable metallic material, zinc alloy releases zinc ions slowly after implantation into bone, so it is necessary to explore the effect of zinc ions on the surrounding tissues. BMSCs are crucial for bone regeneration and osseointegration. The early phases of bone development are marked by the rapid recruitment and adherence of BMSCs, the progenitor cells that give rise to osteoblasts. Therefore, BMSCs are the most commonly used cells in bone biomaterial evaluation. The extracts of pure zinc were diluted to 50 and 10% and the cell viability is measured as in Section 2.2. Cell viability was adversely affected by 100% extracts; when diluted below 50%, there was no adverse effect on cell viability (Figure S1). The Zn^{2+} release profile of pure zinc screws in vitro was detected by ICP−MS (inductively coupled plasma mass spectrometry) (Figure S2). As shown in Figure S2, the zinc ion concentration varied little in the vicinity of 300 μM, which is toxic to cells. When diluted twice, the zinc ion concentration decreases to about 150 μM, which does not have a significant effect on cell viability. To exactly investigate the effects of different concentrations of zinc ions on BMSCs, we designed four different sets of zinc ion concentrations (500, 250, 125, and 50 μM). After treating BMSCs with different concentrations of zinc ions for 24 h, it can be observed that the cell morphology

has changed significantly (Figure 1a). The morphology of BMSCs remains normal at low concentrations of zinc ions (between 50 and 125 μM); at higher concentrations, the density of BMSCs declines and the form of the free spindle becomes circular. In cytoskeleton staining, differences in cell morphology are much more pronounced (Figure 1c). The morphology of the BMSCs was unaffected by low quantities of zinc ions, and the cells were sufficiently stretched to show actin proteins. With the increase in zinc ion concentration, a large number of cytoskeletal proteins were lost, the structure was unclear, the fluorescence signal was weakened, and the nucleus was also reduced in size.

Variations in BMSCs morphology correspond to variations in their viability. Zinc ions had no discernible impact on cell viability at concentrations below 125 μM, but at concentrations over 250 μM, there were more dead cells visible in the live−dead stained pictures (Figure 1b). When the zinc ion concentration hit 500 μM, a significant number of dead cells emerged in the field of vision. The viability remains unaffected at zinc ion concentrations below 125 μM and is more impacted at concentrations of over 250 μM, according to CCK8 tests (Figure 1e). According to the results of CCK8 studies, we discovered that zinc ions have a biphasic effect on BMSCs: at low concentrations (>125 μM), suitable zinc ions promote cell viability, and over the threshold (>250 μM), zinc ions negatively influence the cells, which is consistent with the results of a previous study.[19]

The apoptosis of BMSCs subjected to various zinc ion concentrations was identified by flow cytometric assays (Figure 1d). Similar to the cell activity assay, the results showed that BMSCs were unaffected by zinc ion concentrations below 125 μM (cell survival rates were 97.59, 97.72, and 98.43%, respectively); however, concentrations above 250 μM caused massive apoptosis (cell survival rates dropped to 54.23 and 13.25%), and the rate of apoptosis increased as zinc ion concentrations increased (Figure 1e). Amazingly, when the concentration of zinc ions reached 500 μM, hardly 10% of the BMSCs remained alive.
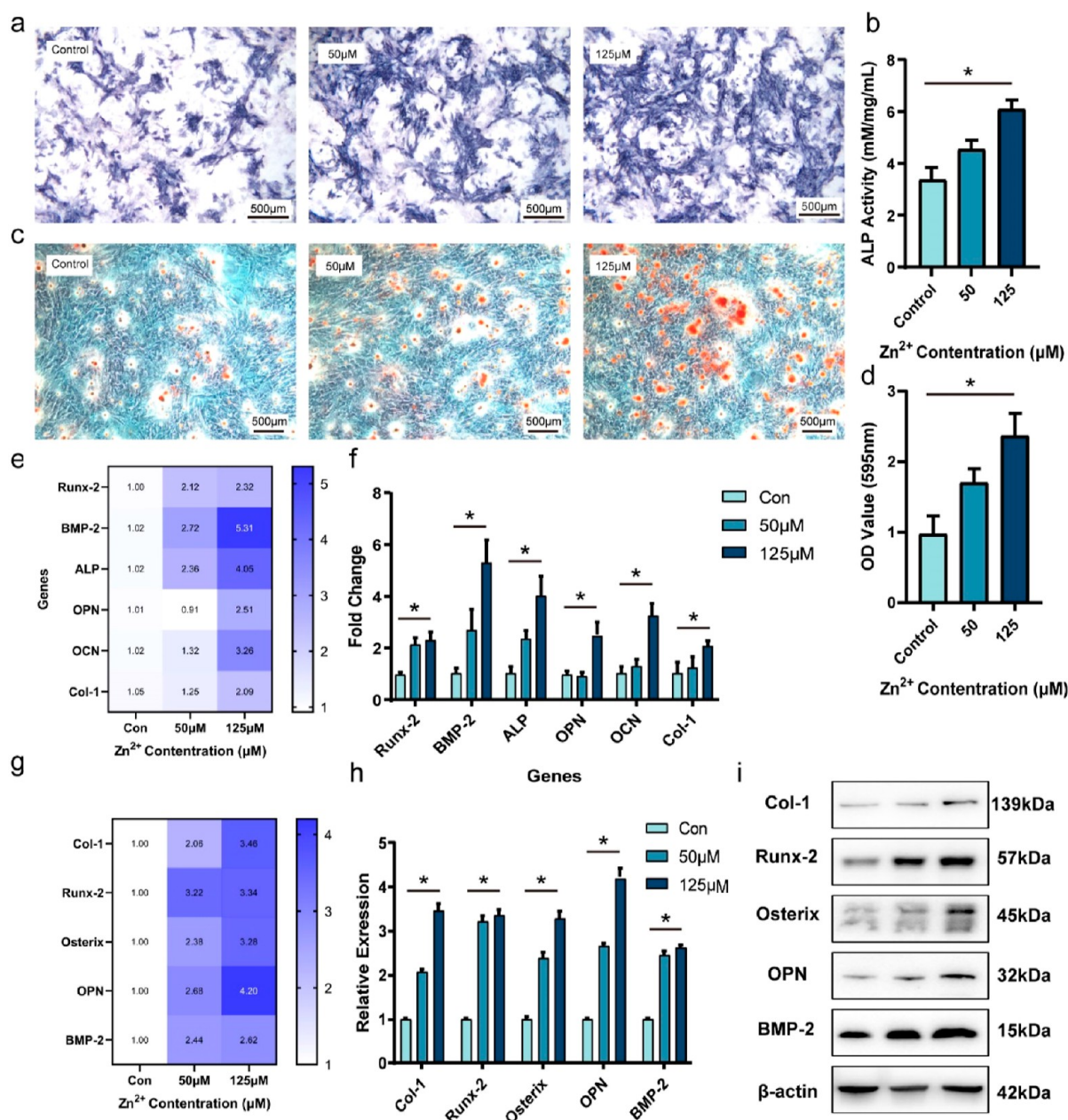
Figure 3. Effect of zinc ions on osteogenic differentiation of BMSCs in vitro. (a) ALP staining. (b) Quantitative analysis of relative ALP activity. (c) Alizarin red (ARS) staining. (d) Quantitative analysis of mineralized calcium deposits. (e) Heatmap of osteogenic-related mRNA expression levels. (f) qRT-PCR of osteogenic-related genes (Runx-2, BMP-2, ALP, OPN, OCN, Col-1). (g) Heatmap of osteogenic-related proteins expression levels. (h) Relative expression levels of osteogenic proteins. (i) Western blot of osteogenic-related proteins (Col-1, Runx-2, Osterix, BMP-2, OPN) (*$P < 0.05$).

Zinc is a trace element that is necessary for humans. Due to its inclusion in over 300 enzymes and an even higher number of other proteins, it is clear how essential it is to human health. Adequate availability of zinc is necessary for proper nucleic acid and protein metabolism, as well as for cell development, division, and function.[20] Therefore, appropriate zinc supplementation facilitates various physiological functions in normal cells. An effective homeostatic mechanism that prevents the buildup of excess zinc is based on cellular zinc. Zinc importer family, which consists of 14 proteins that transport zinc into the cytosol, and zinc transporter family, which consists of 10 proteins that transport zinc out of the cytosol, mediate the cellular homeostasis of zinc.[21] It is unclear exactly how zinc affects apoptosis regulation. Numerous studies show that zinc

may be pro- or antiapoptotic depending on its quantity, and that both excess and deficiency of zinc can cause apoptosis in the same cell line.[22] A zinc-mediated protein activity imbalance brought on by an increase in the intracellular zinc ion concentration impairs cellular function. Moreover, a higher intracellular zinc ion concentration attracts more reactive oxygen species to the mitochondria, lowering the potential of the mitochondrial membrane and causing oxidative stress that damages cells. When constructing orthopedic implants made of zinc alloy, attention should be given to managing the release rate of zinc ions due to the biphasic physiological effects of zinc ions on cells.

3.2. Effects of Different Concentrations of Zinc Ions on Migration of BMSCs. Based on the experiments in
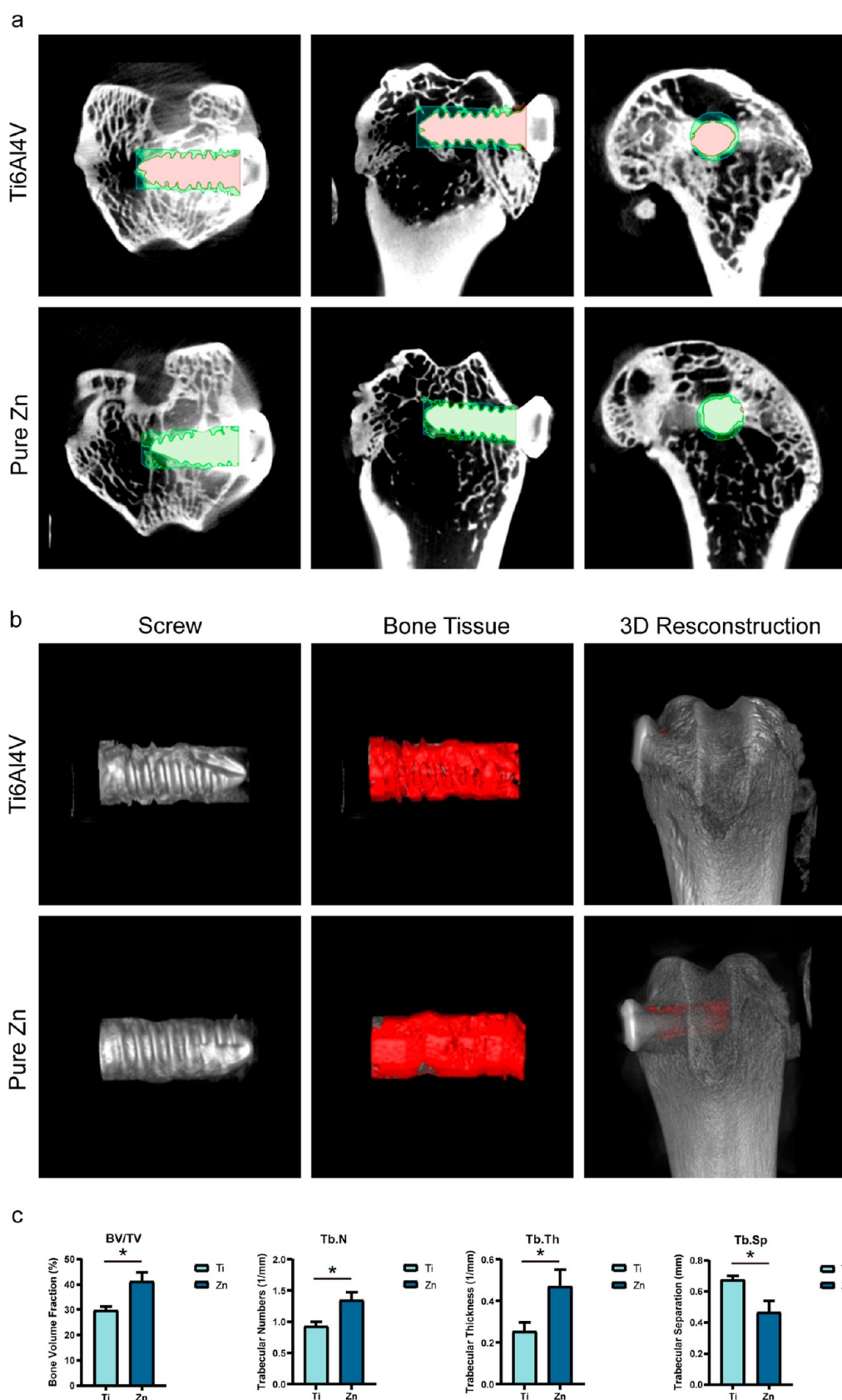
Figure 4. Effect of zinc ions on new bone formation of BMSCs in vivo. (a) Images of microCT scanning. (b) 3D reconstruction images. (c) Quantitative analysis of microCT (*$P < 0.05$).

Section 3.1, it was determined that higher concentrations of zinc ions (>250 μM) would have a negative impact on cell viability. Therefore, in the following study, BMSCs were treated with concentrations of 50 and 125 μM zinc ions to
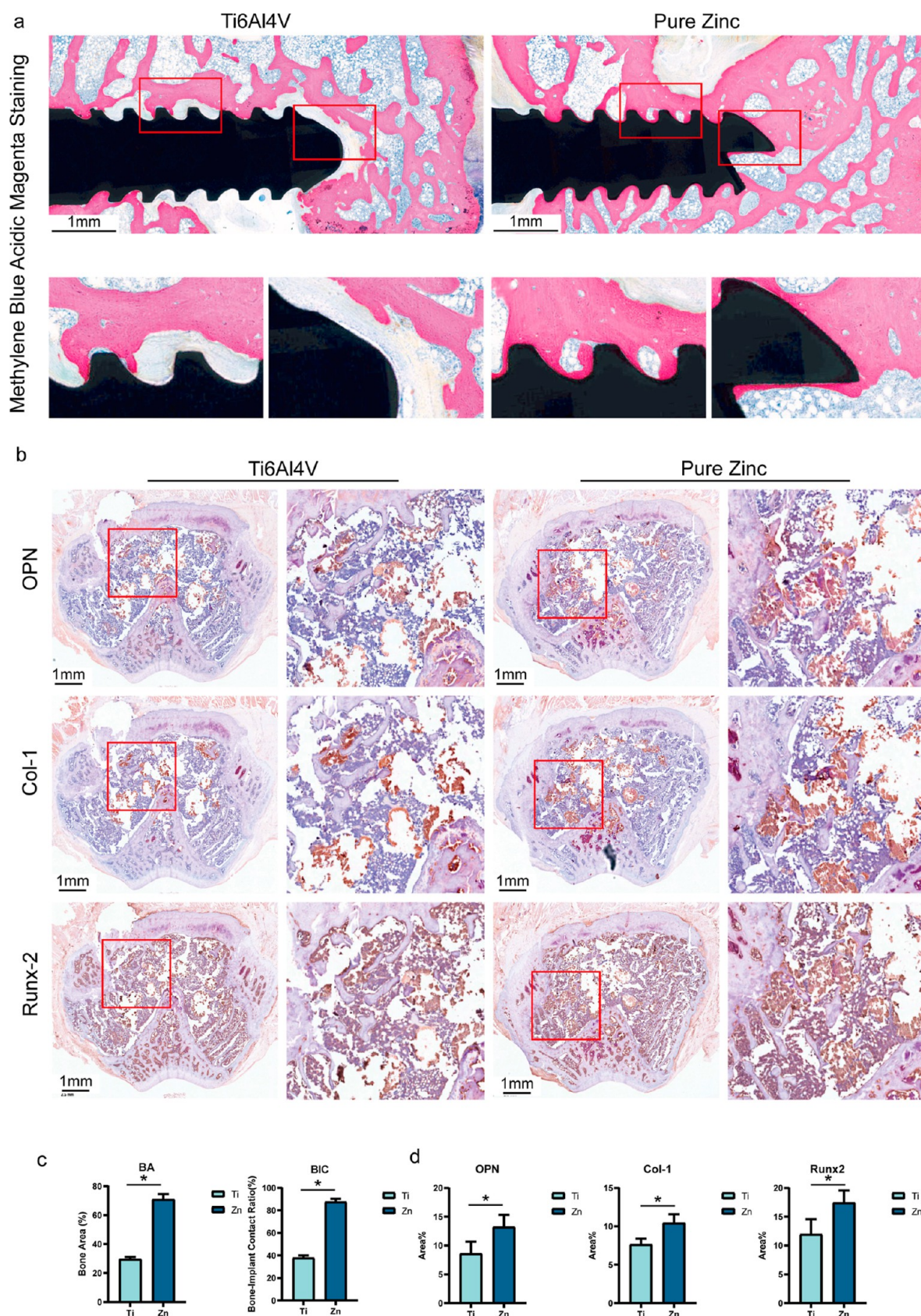
Figure 5. Histological evaluations. (a) Methylene blue acid fuchsin staining of hard-tissue slices. (b) Immunohistochemical staining of OPN, Col-1, and Runx-2. (c) Bone area around the implant (BA) and bone-to-implant contact ratio (BIC). (d) Percentage of immunohistochemical positive staining area ($*P < 0.05$).

examine the impact of zinc ions on the physiological functions of BMSCs. BMSCs were treated with zinc ions for 48 h to assess migration capacity. We found that 50 μM zinc ions had no significant effect on BMSCs migration, while 125 μM zinc ions significantly promoted BMSCs migration (Figure 2a,b).

For a variety of physiological functions, including development, immunological defense, and wound healing, cell migration is necessary. The basic principles of force generation and transfer during cell migration are very consistent—almost all animal cells rely on the dynamics of the "actin cytoskeleton" to move.[23] This set of dynamics can be divided into three actions—adhesion to the substratum, forward actin protrusion, actomyosin contraction, and the formation of the cellular skeleton.[23] It can be hypothesized that appropriate concentrations of zinc ions activate actin function and are more active in migration.

3.3. Effect of Zinc Ions on Osteogenic Differentiation of BMSCs In Vitro. To determine how various zinc ion concentrations impact osteogenic differentiation of BMSCs, we performed in vitro osteogenic evaluations. ALP is a marker of early osteogenic differentiation (7−14 days after osteogenic induction of differentiation) and is often used as one of the criteria for evaluating osteogenic activity. Therefore, ALP levels were initially assessed by staining and activity measurement. The addition of zinc ions increased the staining area and activity of ALP, more significantly in group 125 μM (Figure 3a,b). After a certain amount of time in the presence of induction media, MSCs can differentiate into osteoblasts, which deposit calcium ions on the cell surface and form calcium nodules. The calcium nodule is a late osteogenic differentiation marker (21−27 days after osteogenic induction of differentiation) and can be stained with alizarin red. The Alizarin Red staining and semiquantitative analysis results showed an increase in calcium nodule deposition in the 50 and 125 μM group (Figure 3c,d). Zinc ion supplementation can increase the osteogenic differentiation of BMSCs and the formation of more mineralized calcium nodules in a dose-related manner.

Subsequently, we performed expression assays of osteogenesis-related genes at the mRNA (Figure 3e,f) and protein levels (Figure 3g−i). Both at the transcriptional and translational levels, the addition of zinc ions significantly increased the expression levels of these genes. Runx-2 (Runt-Related Transcription Factor 2), also known as Cbfa1, is a key transcription factor that regulates the differentiation of mesenchymal stem cells toward osteogenesis. Runx-2 regulates the expression of bone ALP, an early gene in osteoblast differentiation, and promotes the differentiation of osteogenic progenitors into osteoblastic precursor cells. Osterix, a gene downstream of Runx-2, is expressed highly specifically in osteoblasts. Osterix et al. determine the differentiation of osteoblast precursors to mature osteoblasts. Bone morphogenetic protein (BMP), belonging to the TGF-β family, activates the downstream Smad1/5/8 signaling pathway after BMP binds to BMP receptors (BMPRs) on the cell surface, phosphorylates Smad1/5/8, and then binds to Smad4 into the nucleus, which regulates the transcription of the BMP target genes, such as Runx-2 and Osterix, and promotes osteoblast differentiation. BMP is required for osteoblast differentiation and bone formation. The results showed that zinc ions effectively increased the expression of key genes in osteogenic differentiation with the greatest impact being shown at a concentration of 125 μM.

3.4. Effect of Zinc Ions on New Bone Formation of BMSCs In Vivo. To further examine the role of zinc ions in stimulating bone regeneration in vivo, we processed pure zinc into bone grafting bare nails and implanted them into the femoral condyles of rats. As a comparison, we utilized titanium alloy (Ti6Al4 V) bone-grafting screws, which are often used in clinical practice. The rat femoral condyles with the implanted titanium or zinc screws were removed after 12 weeks of recovery, and osseointegration and osteogenesis were assessed. First, each group's 3D osteogenesis was assessed by micro-CT analysis (Figure 4a). Under the same threshold and volume of interest for CT scanning, the zinc screws group had a greater formation of new bone compared to the control group (Figure 4b). Additionally, statistical analysis revealed that at 12 weeks postimplantation, the zinc group had substantially greater BV/TV, Tb. N, Tb. Th, and Tb. Sp values than the titanium group (Figure 4c). The zinc screws showed a greater percentage of bone volume to tissue volume, which was consistent with the outcome of osteogenic differentiation in vitro. Zinc screws can release zinc ions gradually upon implantation which is biologically active and stimulates the formation of new bone, as opposed to physiologically inert titanium alloys.

3.5. Histological Evaluations. Following microCT scanning, one portion of the samples underwent the appropriate processing to create hard tissue sections with screws. Using hard tissue histological staining, details of the interfaces between implants and bone were examined. Bone tissue contains a lot of calcium; standard soft tissue sectioning methods necessitate decalcification of the section following implant removal, which damages the tissue's structure and diminishes the importance of observing the tissue. In orthopedic implant research, we are more interested in the morphology of the tissue structure at the implant-bone interface. The hard tissue sectioning approach not only preserves the tissue structure between the implant and the bone interface but also reveals the cellular structure of bone tissue without harming the bone tissue cells, which is a preferable histological test approach. In methylene blue acidic magenta staining (Figure 5a), there was no evidence of fibrous capsule development or foreign-body giant cell formation at the bone-implant interfaces for either of the zinc or titanium screws. More significantly, as shown in Figure 5a, we can see a contiguous bone matrix (pink stain) surrounding the edges of the zinc screws. On the other hand, the titanium screws showed less bone mineral and more fibrous connective tissue (light blue stain). Quantitative analysis (Figure 5c) shows that zinc alloys outperform titanium alloys in the bone area around the implant (BA) and bone-to-implant contact ratio (BIC).

The other portion underwent the appropriate processing to create soft tissue sections without screws and was decalcified. The corresponding protocols were then followed for immunohistochemistry and immunofluorescence staining. Runx-2 can upregulate the expression of Col-1 and OPN, and it is essential in controlling the expression of osteoblast genes. As seen in Figure 5b,d and 6, after 12 weeks, the expression of Runx-2, Col-1, and OPN was significantly greater in the zinc groups compared to the titanium groups.

The following conclusion might be made based on all of these histological findings: in the aspect of promoting osteogenesis, Zn performed better than Ti6Al4 V in terms of osteoblast differentiation and bone matrix mineralization. Compared to biologically inert titanium alloys, the gradual release of zinc ions from biologically active zinc implanted into
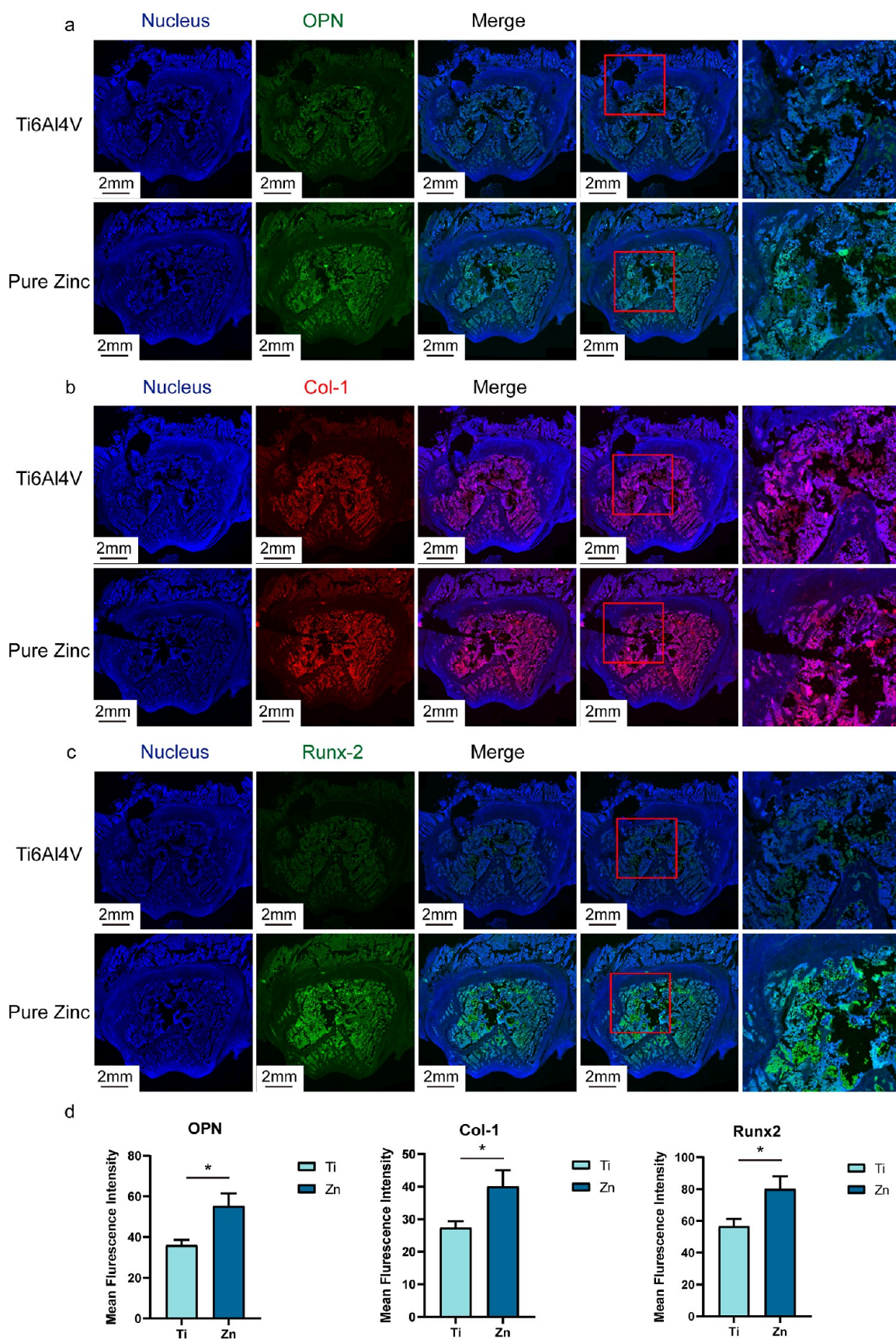
Figure 6. Immunofluorescence staining. (a) Osteopontin staining. (b) Collagen-1 staining. (c) Runt-related transcription factor 2. (d) Semiquantitative analysis of immunofluorescence staining (*$P < 0.05$).
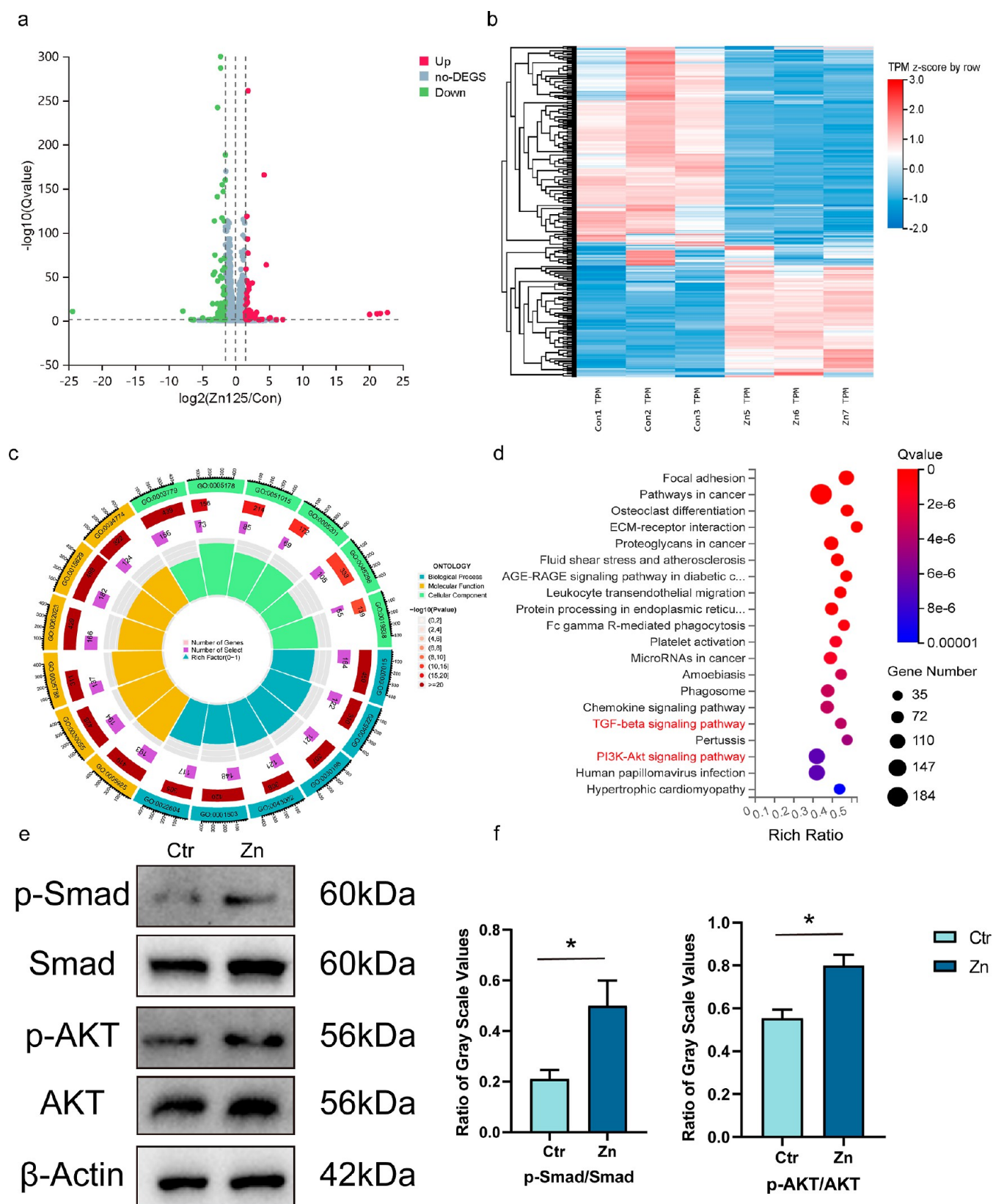
Figure 7. Transcriptome sequencing. (a) Volcano plot displaying the quantity of genes that are downregulated (green dots) and increased (red dots). *P* value < 0.05 and |log 2 FC| > 1. (b) Heat map of DEGs between control and 125 μM zinc ions treated groups. (c) GO analysis revealing the biological roles: molecular function, cellular component, and biological process of DEGs. (d) KEGG pathway enrichment of DEGs. (e) Protein expression levels of *p*-Smad, Smad, *p*-AKT, AKT. (f) Quantification of the gray value of protein bands (**P* < 0.05).

the bone promotes osseointegration and the growth of new bone.

3.6. Transcriptome Sequencing. Given the aforementioned results, zinc ions have been shown to improve

osteogenesis in vivo and in vitro; therefore, we used high-throughput transcriptome sequencing to investigate the underlying molecular mechanisms. After being treated with 125 μM concentration of zinc ions in vitro for 7 days, 75 genes were upregulated and 100 genes were downregulated (Figure 7a,b. cut off: |log 2 FC| ≥ 1.5, Qvalue ≤ 0.05). Gene ontology (GO) enrichment was used to analyze the DEGs (Figure 7c). The majority of these genes are involved in the processes of, including cell proliferation, extracellular matrix organization, and cell adhesion, and so on. Kyoto encyclopedia of genes and genomes (KEGG) enrichment analysis was conducted to identify the important osteogenic signal pathways activated by zinc ions. Two of the top 20 signal pathways (the words in red in Figure 7d) are associated with osteogenesis. As Figure 6d illustrates, zinc ions stimulated TGF-β and PI3K/AKT signaling pathways, which all aid in the osteogenic development of BMSCs.

BMP belongs to the transforming growth factor-β (TGF-β) superfamily. The type I and II receptors dimerize when BMP binds to the type II receptor (BMPRII) and BMPR II binds to the type I receptor (BMPR I). BMPR I is then phosphorylated. The downstream receptor SMADs1/5/8 is recruited and phosphorylated on two serine residues at the C-terminus by the phosphorylated type I receptor. After binding to SMAD4 to create a trimeric complex, the phosphorylated receptor SMAD1/5/8 (pSMAD1/5/8) translocates to the nucleus. The trimeric complex directly controls downstream target gene transcription in the nucleus, including Runx-2.[24] Therefore, we applied Western blot to detect the phosphorylation of smad1/5/8 protein, and the results (Figure 7e,f) showed that the phosphorylation level of smad1/5/8 protein increased after zinc ion treatment, confirming the transcriptome sequencing results.

Phosphoinositide 3-kinase (PI3K)/serine−threonine kinase (Akt) pathway is a crucial signaling route that regulates the bone regenerating process in several systems. It has been demonstrated to be involved in the proliferation and differentiation of osteoblasts.[25] An essential component for both bone production and resorption is the heterodimeric enzyme PI3K. When phosphorylated, PI3K activates Akt, an important downstream protein. Serine/threonine kinase AKT, a proto-oncogene sometimes referred to as protein kinase B or Protein kinase B, PKB, is involved in the control of several cellular processes, including as protein synthesis, growth, proliferation, survival, metabolism, and transcription.[26] Many of AKT's substrates are found in the cytoplasm and nucleus, which it may translocate from the plasma membrane to once activate. By phosphorylation of target proteins, AKT either increases or decreases their activity. As a result, it controls a variety of downstream pathways including osteogenesis related pathways, such as mTOR, VEGF, MAPK, NF-κB, P53, and others.[26] We investigated the phosphorylation level of AKT proteins in light of the crucial role that AKT phosphorylation plays in the route. We found that zinc ions raised the phosphorylation level of AKT proteins (Figure 7e,f), indicating the activation of the mechanism and confirming the sequencing results.

4. CONCLUSIONS

BMSCs are subject to the dual impacts of zinc ions, which vary based on the concentration. On the one hand, because of the disrupted zinc homeostasis and excessive Zn^{2+} excess, the extremely high concentration of zinc ions (>250 μM) not only decreases the viability and proliferation of BMSCs but also causes BMSCs to undergo apoptosis. On the other hand, the low concentration of Zn^{2+} (125 μM) can efficiently promote the cell viability, proliferation, and migration and further induce the osteogenic differentiation of BMSCs by triggering the TGF-β and PI3K-AKT-signaling pathway. When designing biodegradable zinc orthopedic implants, care should be taken to control the rate of release of zinc ions for pro-bone regenerative effects.

■ ASSOCIATED CONTENT

Ⓢ Supporting Information

The Supporting Information is available free of charge at https://pubs.acs.org/doi/10.1021/acsomega.3c10344.

> The extractions of pure zinc screw samples were obtained by incubating equal mass (1 g) in 10 mL of α-MEM media for 24 h and then filtering with 0.22 μm filters, and the extracts were diluted to 50 and 10% and the cell viability is measured. Figure S1 shows the effect of different concentrations of extracts on cell viability. According to ASTM G31-12a, immersion test was performed in SBF solution for 168 h. Pure zinc samples with a surface area of 3 cm^2 were immersed in 60 mL of SBF solution at 37 °C, and then the SBF solution was renewed every 48 h. The concentration of zinc ions in the SBF were detected by ICP−MS (inductively coupled plasma mass spectrometry) every day. The zinc ion release profile is shown in Figure S2 (PDF)

■ AUTHOR INFORMATION

Corresponding Authors

Bin Zhu − Department of Orthopaedics, Beijing Friendship Hospital, Capital Medical University, Beijing 100050, P. R. China; Email: zhubin@bjmu.edu.cn

Xiaoguang Liu − Department of Orthopaedics, Peking University Third Hospital, Beijing 100191, P. R. China; Beijing Key Laboratory of Spinal Disease Research, Beijing 100191, P. R. China; Engineering Research Center of Bone and Joint Precision Medicine, Ministry of Education, Beijing 100191, P. R. China; ⓞ orcid.org/0000-0002-5663-5238; Email: xgliuspine@sina.com

Authors

Yu Liu − Department of Orthopaedics, Peking University Third Hospital, Beijing 100191, P. R. China; Beijing Key Laboratory of Spinal Disease Research, Beijing 100191, P. R. China; Engineering Research Center of Bone and Joint Precision Medicine, Ministry of Education, Beijing 100191, P. R. China; ⓞ orcid.org/0000-0001-5930-3960

Linbang Wang − Department of Orthopaedics, Peking University Third Hospital, Beijing 100191, P. R. China; Beijing Key Laboratory of Spinal Disease Research, Beijing 100191, P. R. China; Engineering Research Center of Bone and Joint Precision Medicine, Ministry of Education, Beijing 100191, P. R. China

Xinyu Dou − Department of Orthopaedics, Peking University Third Hospital, Beijing 100191, P. R. China; Beijing Key Laboratory of Spinal Disease Research, Beijing 100191, P. R. China; Engineering Research Center of Bone and Joint Precision Medicine, Ministry of Education, Beijing 100191, P. R. China

Mingze Du − *Department of Sports Medicine, Peking University Third Hospital, Beijing 100191, P. R. China; Beijing Key Laboratory of Sports Injuries, Beijing 100191, P. R. China; Engineering Research Center of Sports Trauma Treatment Technology and Devices, Ministry of Education, Beijing 100191, P. R. China*

Shuyuan Min − *Department of Orthopaedics, Peking University Third Hospital, Beijing 100191, P. R. China; Beijing Key Laboratory of Spinal Disease Research, Beijing 100191, P. R. China; Engineering Research Center of Bone and Joint Precision Medicine, Ministry of Education, Beijing 100191, P. R. China*

Complete contact information is available at:
https://pubs.acs.org/10.1021/acsomega.3c10344

Author Contributions

Y.L. contributed to the conceptualization, methodology, writing—original draft, and writing—review and editing. L.W. contributed to methodology and writing—original draft. X.D. and M.D. contributed to data curation and methodology. S.M. contributed to formal analysis. B.Z. contributed to supervision, project administration, and writing—review and editing. X.L. contributed to supervision, project administration, writing—review and editing, and funding acquisition.

Notes

The authors declare no competing financial interest.

■ REFERENCES

(1) Hernández-Escobar, D.; Champagne, S.; Yilmazer, H.; Dikici, B.; Boehlert, C. J.; Hermawan, H. Current status and perspectives of zinc-based absorbable alloys for biomedical applications. *Acta Biomater.* **2019**, *97*, 1−22.

(2) Wang, J.-L.; Xu, J.-K.; Hopkins, C.; Chow, D. H.-K.; Qin, L. Biodegradable Magnesium-Based Implants in Orthopedics-A General Review and Perspectives. *Advanced Science* **2020**, *7* (8), 1902443.

(3) Kabir, H.; Munir, K.; Wen, C.; Li, Y. Recent research and progress of biodegradable zinc alloys and composites for biomedical applications: Biomechanical and biocorrosion perspectives. *Bioact. Mater.* **2021**, *6* (3), 836−879.

(4) Su, Y.; Cockerill, I.; Wang, Y.; Qin, Y.-X.; Chang, L.; Zheng, Y.; Zhu, D. Zinc-Based Biomaterials for Regeneration and Therapy. *Trends Biotechnol.* **2019**, *37* (4), 428−441.

(5) Seitz, J.-M.; Lucas, A.; Kirschner, M. Magnesium-Based Compression Screws: A Novelty in the Clinical Use of Implants. *JOM* **2016**, *68* (4), 1177−1182.

(6) Bowen, P. K.; Drelich, J.; Goldman, J. Zinc Exhibits Ideal Physiological Corrosion Behavior for Bioabsorbable Stents. *Adv. Mater.* **2013**, *25* (18), 2577−2582.

(7) Liu, H.; Zhang, X.; Liu, J.; Qin, J. Vascularization of engineered organoids. *Biomed. Mater. Eng.* **2023**, *1* (3), No. e12031.

(8) Maret, W. Zinc biochemistry: from a single zinc enzyme to a key element of life. *Adv. Nutr.* **2013**, *4*, 82−91.

(9) Jiang, X.; Zhang, W.; Terry, R.; Li, W. The progress of fabrication designs of polymeric microneedles and related biomedical applications. *Biomed. Mater. Eng.* **2023**, *1* (4), No. e12044.

(10) Jin, G.; Cao, H.; Qiao, Y.; Meng, F.; Zhu, H.; Liu, X. Osteogenic activity and antibacterial effect of zinc ion implanted titanium. *Colloids Surf., B* **2014**, *117*, 158−165.

(11) Saino, E.; Grandi, S.; Quartarone, E.; Maliardi, V.; Galli, D.; Bloise, N.; Fassina, L.; De Angelis, M. G. C.; Mustarelli, P.; Imbriani, M.; Visai, L. In vitro calcified matrix deposition by human osteoblasts onto a zinc-containing bioactive glass. *Eur. Cells Mater.* **2011**, *21*, 59−72.

(12) Huo, K.; Zhang, X.; Wang, H.; Zhao, L.; Liu, X.; Chu, P. K. Osteogenic activity and antibacterial effects on titanium surfaces modified with Zn-incorporated nanotube arrays. *Biomaterials* **2013**, *34*, 3467−3478.

(13) Venezuela, J.; Dargusch, M. S. The influence of alloying and fabrication techniques on the mechanical properties, biodegradability and biocompatibility of zinc: A comprehensive review. *Acta Biomater.* **2019**, *87*, 1−40.

(14) Yang, H.; Jia, B.; Zhang, Z.; Qu, X.; Li, G.; Lin, W.; Zhu, D.; Dai, K.; Zheng, Y. Alloying design of biodegradable zinc as promising bone implants for load-bearing applications. *Nat. Commun.* **2020**, *11* (1), 401.

(15) Chen, C.; Bu, W.; Ding, H.; Li, Q.; Wang, D.; Bi, H.; Guo, D. A.-O. Cytotoxic effect of zinc oxide nanoparticles on murine photoreceptor cells via potassium channel block and Na(+)/K(+)-ATPase inhibition. *Cell Proliferation* **2017**, *50*, No. e12339.

(16) Arakha, M.; Roy, J.; Nayak, P. S.; Mallick, B.; Jha, S. Zinc oxide nanoparticle energy band gap reduction triggers the oxidative stress resulting into autophagy-mediated apoptotic cell death. *Free Radical Biol. Med.* **2017**, *110*, 42−53.

(17) Chen, X.; Wang, J.; Yu, L.; Zhou, J.; Zheng, D.; Zhang, B. Effect of Concentrated Growth Factor (CGF) on the Promotion of Osteogenesis in Bone Marrow Stromal Cells (BMSC) in vivo. *Sci. Rep.* **2018**, *8* (1), 5876.

(18) Jia, B.; Yang, H.; Han, Y.; Zhang, Z.; Qu, X.; Zhuang, Y.; Wu, Q.; Zheng, Y.; Dai, K. In vitro and in vivo studies of Zn-Mn biodegradable metals designed for orthopedic applications. *Acta Biomater.* **2020**, *108*, 358−372.

(19) Yu, Y.; Liu, K.; Wen, Z.; Liu, W.; Zhang, L.; Su, J. Double-edged effects and mechanisms of Zn(2+) microenvironments on osteogenic activity of BMSCs: osteogenic differentiation or apoptosis. *R. Soc. Chem.* **2020**, *10*, 14915−14927.

(20) Plum, L. M.; Rink, L.; Haase, H. The Essential Toxin: Impact of Zinc on Human Health. *Int. J. Environ. Res. Public Health* **2010**, *7* (4), 1342−1365.

(21) Lichten, L. A.; Cousins, R. J. Mammalian zinc transporters: nutritional and physiologic regulation. *Annu. Rev. Nutr.* **2009**, *29*, 153−176.

(22) Formigari, A.; Irato, P.; Santon, A. Zinc, antioxidant systems and metallothionein in metal mediated-apoptosis: biochemical and cytochemical aspects. *Comparative Biochemistry and Physiology Part C: Toxicology & Pharmacology* **2007**, *146*, 443−459.

(23) Yamada, K. M.; Sixt, M. Mechanisms of 3D cell migration. *Nat. Rev. Mol. Cell Biol.* **2019**, *20*, 738−752.

(24) Zieba, J. T.; Chen, Y.-T.; Lee, B. H.; Bae, Y. J. Notch Signaling in Skeletal Development, Homeostasis and Pathogenesis. *Biomolecules* **2020**, *10* (2), 332.

(25) Wang, T.; Zhang, X.; Bikle, D. D. Osteogenic Differentiation of Periosteal Cells During Fracture Healing. *J. Cell. Physiol.* **2017**, *232* (5), 913−921.

(26) Dong, K.; Zhou, W.-J.; Liu, Z.-H.; Hao, P.-J. The extract of concentrated growth factor enhances osteogenic activity of osteoblast through PI3K/AKT pathway and promotes bone regeneration in vivo. *Int. J. Implant Dent.* **2021**, *7* (1), 70.